BVRI Photometric Study of the High Mass Ratio, Detached, Pre-contact W UMa Binary GQ Cancri

Ronald G. Samec
Amber Olson
Natural Sciences Department, Emmanuel College, 181 Springs Street, Franklin Springs, GA 30639; ronaldsamec@gmail.com

Daniel Caton
Dark Sky Observatory, Department of Physics and Astronomy, Appalachian State University, 525 Rivers Street, Boone, NC 28608

Danny R. Faulkner
Johnson Observatory, 1414 Bur Oak Court, Hebron, KY 41048

Walter Van Hamme
Department of Physics, Florida International University, 11200 SW 8th Street, CP 204, Miami, FL 33199

Received June 30, 2017; revised August 8, August 18, 2017; accepted August 18, 2017

Abstract CCD BVR_cI_c light curves of GQ Cancri were observed in April 2013 using the SARA North 0.9-meter Telescope at Kitt Peak National Observatory in Arizona in remote mode. It is a high-amplitude (V ~ 0.9 magnitude) K0–V type eclipsing binary (T_1 ~ 5250 K) with a photometrically-determined mass ratio of $M_2 / M_1 = 0.80$. Its spectral color type classifies it as a pre-contact W UMa Binary (PCWB). The Wilson-Devinney Mode 2 solutions show that the system has a detached binary configuration with fill-outs of 94% and 98% for the primary and secondary component, respectively. As expected, the light curve is asymmetric due to spot activity. Three times of minimum light were calculated, for two primary eclipses and one secondary eclipse, from our present observations. In total, some 26 times of minimum light covering nearly 20 years of observation were used to determine linear and quadratic ephemerides. It is noted that the light curve solution remained in a detached state for every iteration of the computer runs. The components are very similar with a computed temperature difference of only 4 K, and the flux of the primary component accounts for 53–55% of the system's light in B, V, R_c, and I_c. A 12-degree radius high latitude white spot (faculae) was iterated on the primary component.

1. Introduction

Contact binaries with mass ratios near unity are very rare. In this study, we analyze a near contact solar type binary (a pre-contact W UMa binary) with a mass ratio near that of unity. The Wilson-Devinney (WD) program was used for this calculation. This paper represents the first precision BVR_cI_c study of GQ Cnc. A mass ratio (q) search was needed since a number of solutions may be generated with different values of q. However, in this case, the deep, knife-like, nearly identical eclipses are possible only when q is near one.

The formation of contact binaries may happen in one of three evolutionary channels (Jiang *et al.* 2014). One is nuclear expansion of the primary component, two others involve loss or exchange of angular momentum via magnetic braking or by interacting with a third body. Magnetic braking occurs since solar type stars are highly magnetic in nature, due to their convective envelopes and fast rotation. They undergo magnetic braking as plasma winds leave the stars on stiff rotating dipole fields. This action torques the binary, eventually bringing them into contact and finally, following a red novae event (Molnar *et al.* 2017), leaves a single, fast-rotating star.

2. History and observations

The variable NSV 4411 (GQ Cnc) was discovered by Rigollet (1953) and classified as a RR Lyrae variable star with a photographic magnitude of 13.1 to 13.7. It was observed in 1996 with a CCD camera (Vidal-Sainz and Garcia-Melendo 1996) and found to be an eclipsing binary with an ephemeris of:

$$\text{Min. I.} = \text{HJD } 2450154.2091 + 0.42228 \text{ d} \times E. \quad (1)$$

They gave seven eclipse timings in their paper. Their light curve fit (BINARY MAKER 2.0; Bradstreet 1993) gave a mass ratio of 0.9 and an inclination of 86° and a component temperature difference of 150 K. They included a cool spot on the primary component. Their V filter CCD curve is given as Figure 1.

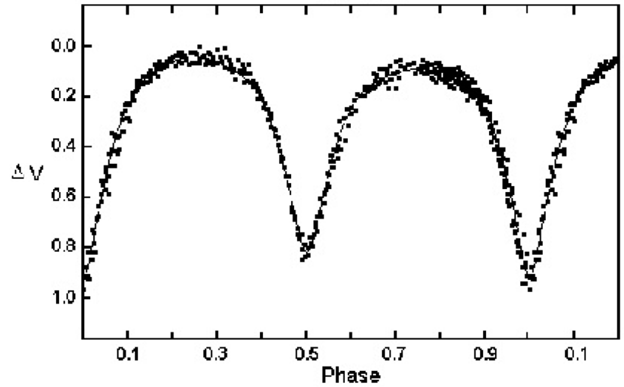

Figure 1. V-filtered CCD Light curve (Vidal-Sainz and Garcia-Melendo 1996).

Table 1. Information on the stars used in this study.

Star	*Name*	*R.A. (2000)* h m s	*Dec. (2000)* ° ′ ″	*V*	*J–K*	*B–V*
V	GQ Cnc 3UC234-096892* 2MASS J09120836+2650180 NSV 4411 GSC 01954 00180	09 12 08.386	+26 50 18.20[1]	12.96	0.51	0.81
C	BD +27.1722	09 12 23.58	+26 52 44.6[2]	9.76	—	0.815
K (Check)	TYCHO 1954 642	09 12 08.7879	+26 46 33.966[3]	10.622	0.625 (K3)	1.006 (K4)

[1] *UCAC3 (USNO 2012).* [2] *Perryman et al. (1997).* [3] *Høg, E., et al. (2000).*

GQ Cnc was included in the "75th Name-list of Variable Stars" (Kazarovets *et al.* 2000). Times of minimum light are given by Hübscher and Monninger (2011), Zejda (2004), Diethelm (2003, 2012, 2010, 2009), and Locher (2005). An updated ephemeris was given by Kreiner (2004):

$$\text{Min. I.} = \text{HJD } 2452500.0108\ (4) + 0.4222087\ \text{d}\ (1) \times E. \quad (2)$$

It is listed in the automated variable star classification using the NSVS (Hoffman *et al.* 2009) as an Algol/EB type and W UMa, with a period of 0.42221 day and J–H = 0.396, H–K = 0.114, a ROTSE magnitude of 12.702, and an amplitude of 0.865. It is listed in the Fourier region where β Lyr stars are expected (http://vizier.u-strasbg.fr/viz-bin/VizieR).

CCD BVR_cI_c light curves of GQ Cnc were observed in April 2013 on the SARA North 0.9-meter Telescope at Kitt Peak National Observatory in Arizona in remote mode by Samec with a –110° C cooled 2 K × 2 K, ARC-E2V42-40 chip CCD camera. Standard B, V, R_c, and I_c Johnson-Cousins filters were used. Reduction and analyses were mostly done by authors Samec, Olson, and Caton. Individual observations included 203 in B, 236 in V, 259 in R, and 260 in I. The standard error of a single observation was ~14 mmag. in B, 12 mmag. in V, 8 mmag. in R, and 9 mmag. in I. Images were calibrated from biases, 10–300-second darks and a minimum of five B, V, R_c, and I_c flat frames taken nightly. The nightly C–K values stayed constant throughout the observing run with a precision of 1%. Exposure times varied from 250–275 seconds in B, 80–100 seconds in V, and 30–50 seconds in R_c and I_c.

3. Finding charts and stellar identifications

The finding chart, given here for future observers, is shown as Figure 2. The coordinates and magnitudes of the variable star, comparison star, and check star are given in Table 1. The C–K values stayed constant throughout the observing run to better than 1%. Figures 3 and 4 show sample observations of B, V, and B–V color curves on the night of 24 April 2013, and R_c, I_c, and R_c–I_c color curves on 8 April 2013. Our observations are given in Table 2, in delta magnitudes, ΔB, ΔV, ΔR_c, and ΔI_c, in the sense of variable minus comparison star.

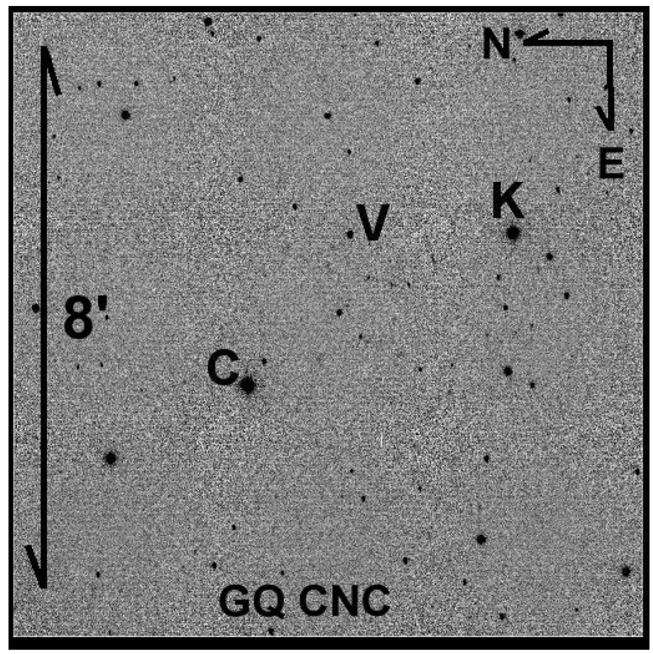

Figure 2. Finder chart for GQ Cnc. V: variable star, C: comparison star, K: check star.

4. Period study

Three times of minimum light were calculated for two primary eclipses and one secondary eclipse from our present observations with the Kwee van Woerden (1956) method:

$$\text{HJD I} = 2456390.66196 \pm 0.00002,\ 2456406.7056 \pm 0.0001 \quad (1)$$

$$\text{HJD II} = 2456405.6505 \pm 0.0002 \quad (2)$$

In total, some 26 times of minimum light covering 17 years of observation (Table 3) were used to determine the following linear ephemeris:

$$\text{HJD MinI} = 2456406.7057 \pm 0.0007 + 0.422208807 \pm 0.00000074\ \text{d} \times E \quad (3)$$

A negative quadratic ephemeris was also calculated:

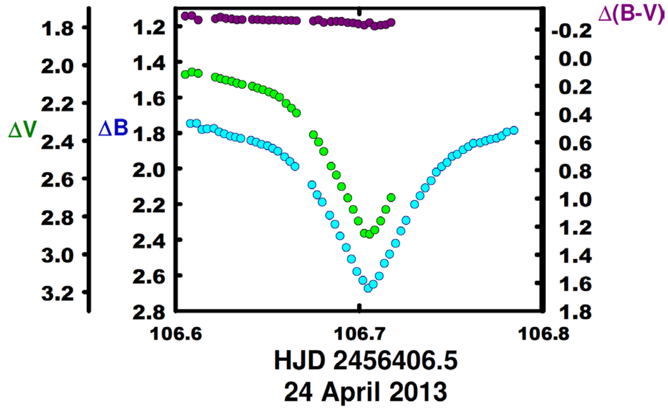

Figure 3. GQ Cnc B, V observations from 24 April 2013.

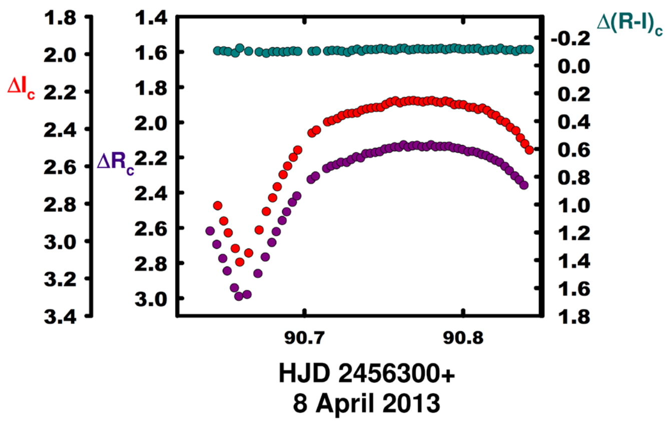

Figure 4. GQ Cnc R_c, I_c observations from 8 April 2013.

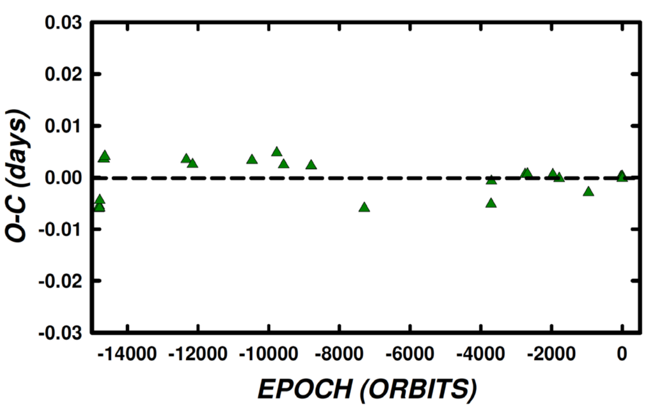

Figure 5. O–C residuals from the linear ephemeris of GQ Cnc from equation (3).

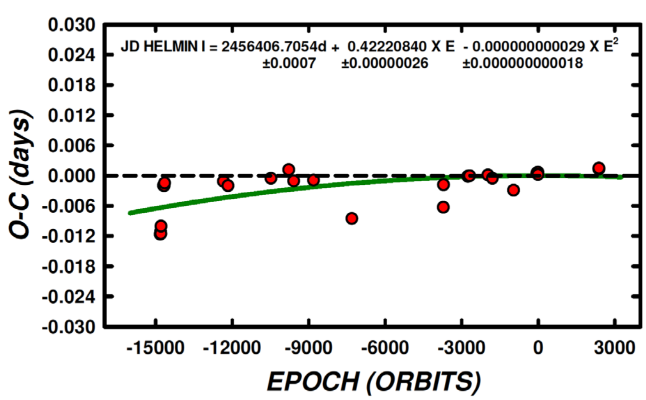

Fiigure 6. O–C Residuals from the quadratic term compared to the linear terms of GQ Cnc from equation (4). This shows that the period may be slowly decreasing at a rate near that theoretically expected for magnetic braking (for example, Molnar *et al.* 2017).

$$\text{HJD Min I} = 2456406.7054\text{d} + 0.42220840 \pm 0.0007 \pm 0.00000026 \times E - 2.9 \times 10^{-11} \pm 1.8 \times 10^{-11} \times E^2. \quad (4)$$

The O–C residuals, both linear and quadratic calculations, are given in Table 3. The linear and quadratic residuals are shown in Figures 5 and 6. The rms residuals for the linear and quadratic ephemerides were 1.15×10^{-5} and 1.13×10^{-5}, respectively. This means that both are very similar and no conclusion may be made of which best describes the data.

The light curves phased using equation (3) of GQ Cnc, delta mag vs. phase, are shown in Figures 7 and 8. Light curve amplitudes and the differences in magnitudes at various quadratures are given in Table 4.

5. Light curve characteristics

The light curves are of good precision, 0.014 magnitude in ΔB, 0.011 in ΔV, 0.008 in ΔR_c, and 0.009 in ΔI_c. The amplitude of the light curve is ~ 0.85 magnitude in all filters. This is quite large for a W UMa binary. This could mean the inclination is high and/or the mass ratio is near unity. The O'Connell effect, which is classically an indication of spot activity, varies 3–4%. This means that solar type spots are probably active, as expected. The differences in minima are small, 0.08 magnitude in all filters, pointing to the nearly equal temperatures of the components.

6. Temperature and light curve solution

2MASS (Skrutskie *et al.* 2006) gives J–K = 0.51 (K0V) or a temperature ~ 5250 K (Cox 2000), which was used in the light curve solution. This is a typical temperature of a short period (< 0.3 d) W UMa contact binary. This gives us a hint that we are observing a precursor to a W UMa Binary and that the evolution is following a detached to contact channel (Jiang *et al.* 2014).

The B, V, R_c, and I_c light curves were carefully pre-modeled with BINARY MAKER 3.0 (Bradstreet and Steelman 2002) and light curve fits were determined in all filter bands. The hand modeling revealed that both semidetached and detached models would fit the data (both with spots). The parameters from these two results were then averaged and input into a four-color simultaneous light curve calculation using the Wilson-Devinney (WD) program (Wilson and Devinney 1971; Wilson 1990, 1994; Van Hamme and Wilson 1998). The present solution was computed in Mode 2; which allows WD to determine the configuration. Convective parameters, g = 0.32, A = 0.5, were used. The program iterations remained and converged in a detached configuration. A mass ratio very nearly unity was determined with the first solution. We preserve this computation by including it in Table 5 (q = 0.95). Iterated parameters included both surface potentials, mass ratio, all spot parameters, inclination, T_2 (T_1 fixed), the ephemeris, and the relative monochromatic luminosity (L_1). Both a hot spot and a dark spot were used in BINARY MAKER modeling, but only a white spot (faculae) persisted in the WD modeling. Next we determined solutions with q-values fixed and noted the sum of square residuals given by the program for each. We show the

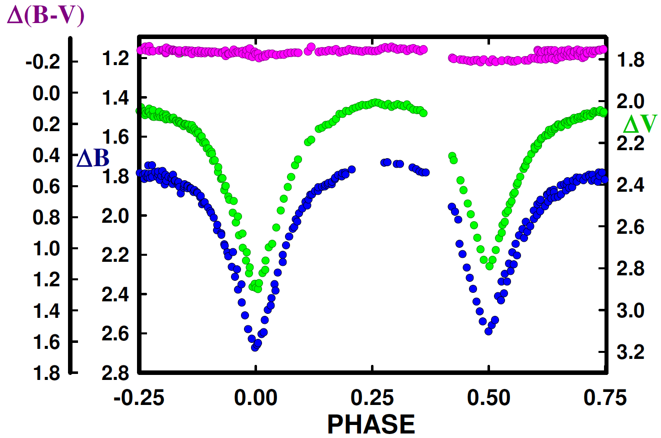

Figure 7. B, V phases calculated from Equation 3.

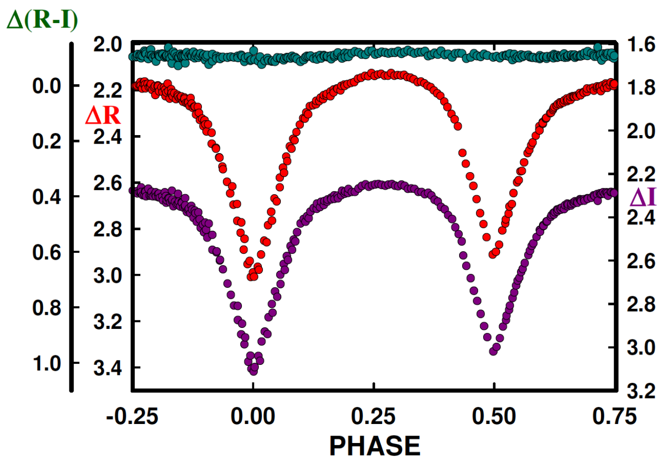

Figure 8. R_c, I_c phases calculated from Equation 3.

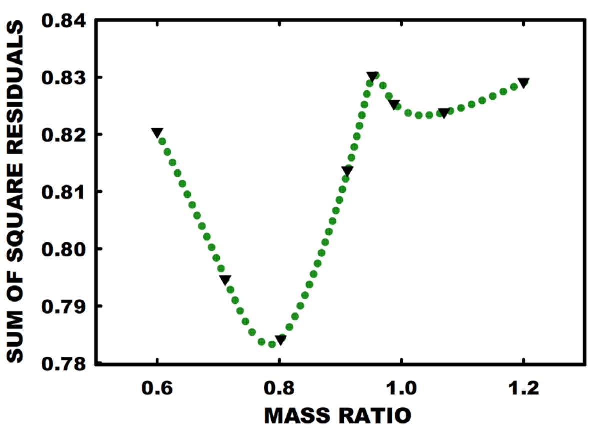

Figure 9. Goodness-of-fit values versus various values of mass ratio (q). The residual minimizes at about 0.8.

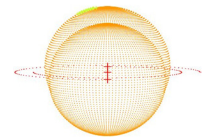

Figure 10a. Geometrical representation at phase 0.00 of GQ Cnc.

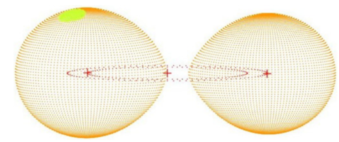

Figure 10b. Geometrical representation at phase 0.25 of GQ Cnc.

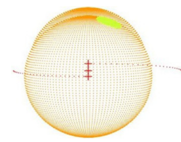

Figure 10c. Geometrical representation at phase 0.50 of GQ Cnc.

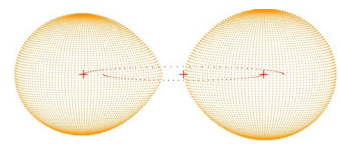

Figure 10d. Geometrical representation at phase 0.75 of GQ Cnc.

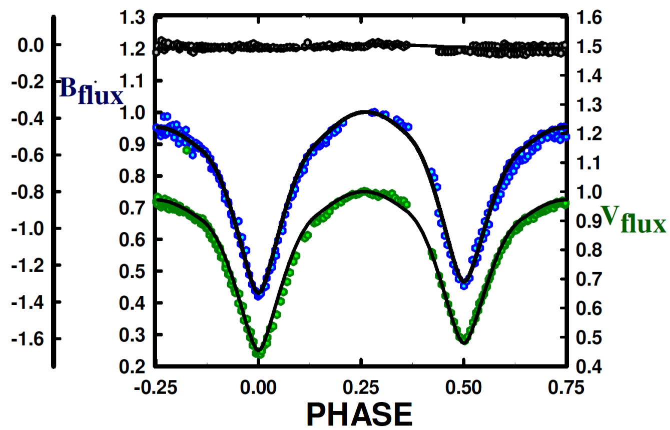

Figure 11a. B,V normalized fluxes overlaid by our solution of GQ Cnc.

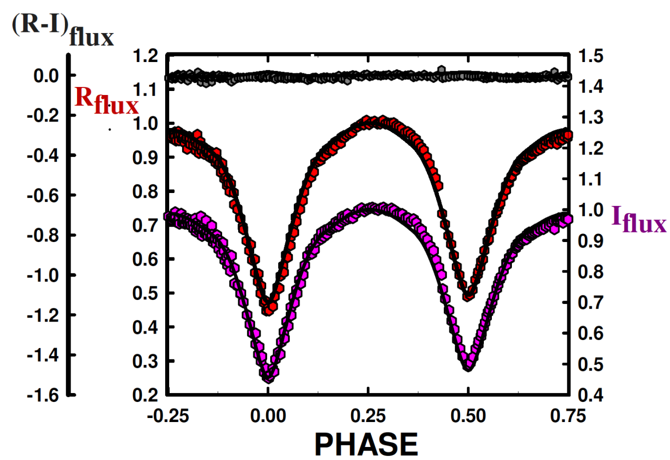

Figure 11b. R_c,I_c normalized fluxes overlaid by our solution of GQ Cnc.

results of that analysis in Figure 9. The best solution occurred at about q = 0.8. This was surprising since we thought the mass ratio would be nearer unity due to the near equal temperatures. A geometrical (Roche-lobe) representation of the system is given in Figure 10 (a, b, c, d) at the light curve quadratures so that the reader may see the placement of the spot and the relative size of the stars as compared to the orbit. As seen, the system is detached. The normalized curves overlain by our light curve solutions are shown as Figures 11a and 11b.

7. Discussion

Our model of GQ Cnc is a precontact W UMa binary. In addition, the stars are virtually the same in temperature. Since contact is not yet attained, we suspect the components began as nearly identical stars. The components' temperatures are within 4 K of each other. The mass ratio is 0.80, even though the fill-outs are nearly identical, 97 and 99% for the primary and secondary components, respectively. This may indicate that component 2 is slightly more evolved than component 1. The lights, 53% and

47%, for the primary and secondary components, respectively, are very similar. Even though the stars are near duplicates of each other, the curves are not symmetrical, with distortions that are probably due to spots. This betrays the fact that the nature of these are solar type, magnetic stars. Contact W UMa binaries with the $q > 0.72$ are called H-subtype systems (Csizmadia and Klagyivik 2004). GQ Cnc may be a precursor of this type of contact binary. Extreme examples of this subtype of contact binary are V803 Aql (Samec *et al.* 1993) and WZ And (Zhang and Zhang 2006), with mass ratios equal to unity.

8. Conclusion

GQ Cnc is apparently approaching contact for the first time with a mass ratio near unity and fill-outs less than critical contact. Solar type binaries, over time, should steadily lose angular momentum and spin down as the ion winds stream outward on stiff magnetic field lines rotating with the binary (out to the Alfvén radius). The natural tendency is for mass ratios to become more extreme with time (move away from unity) and coalesce into a contact binary. The system evidently will come into contact as a H sub-type W UMa binary (mass ratio > 0.72). Ultimately, one expects the binary will coalesce, producing a rather normal, fast rotating, single F2V-type ($m = 1.5\,M_\odot$) field star, assuming a $0.1\,M_\odot$ mass loss. The weakly negative quadratic ephemeris found in the period study may indicate that the binary is following this pattern.

9. Future work

Radial velocity curves are needed to obtain absolute (not relative) system parameters, including a firm determination of the mass ratio. Continued monitoring of eclipses could confirm or disaffirm the period evolution scenario given here.

10. Acknowledgements

Dr. Samec wishes to thank Emmanuel College and its vice president, Dr. John Henzel, President for Academic Affairs, for their past support for travel, and membership fees and meeting expenses.

References

Blättler, E., Diethelm, R., and Guilbault, P. 2001, *BBSAG Bull.*, No. 125, 1.
Bradstreet, D. H. 1993, in *Light Curve Modeling of Eclipsing Binary Stars*, IAU Symp. 151, Springer-Verlag, Berlin, 151.
Bradstreet, D. H., and Steelman, D. P. 2002, *Bull. Amer. Astron. Soc.*, **34**, 1224.
Cox, A. N., ed. 2000, *Allen's Astrophysical Quantities*, 4th ed., Springer, New York.
Csizmadia, Sz., and Klagyivik, P. 2004, *Astron. Astrophys.*, **426**, 1001.
Diethelm, R. 2003, *Inf. Bull. Var. Stars*, No. 5438, 1.
Diethelm, R. 2009, *Inf. Bull. Var. Stars*, No. 5894, 1.
Diethelm, R. 2010, *Inf. Bull. Var. Stars*, No. 5945, 1.
Diethelm, R. 2012, *Inf. Bull. Var. Stars*, No. 6029, 1.
Høg, E., *et al.* 2000, *Astron. Astrophys.*, **355**, L27.
Hoffman, D. I., Harrison, T. E., and McNamara, B. J. 2009, *Astron. J.*, **138**, 466.
Hübscher, J. 2017, *Inf. Bull. Var. Stars*, No. 6196, 1.
Hübscher, J., and Monninger, G. 2011, *Inf. Bull. Var. Stars*, No. 5959, 1.
Jaing, D., Han, Z., and Lifang, L. 2014, *Mon. Not. Roy. Astron. Soc.*, **438**, 859.
Kazarovets, E. V., Samus, N. N., and Durlevich, O. V. 2000, *Inf. Bull. Var. Stars*, No. 4870, 1.
Kreiner, J. M. 2004, *Acta Astron.*, **54**, 207.
Kwee, K. K., and van Woerden, H. 1956, *Bull. Astron. Inst. Netherlands*, **12**, 327.
Locher, K. 2005, *Open Eur. J. Var. Stars*, **3**, 1.
Locher, K., Blättler, E., and Diethelm, R. 2002, *BBSAG Bull.*, No. 128, 1.
Molnar, L. A., *et al.* 2017, *Astrophys. J.*, **840**, 1.
Paschke, A. 1999, observation of GQ Cnc in O–C Gateway (http://var2.astro.cz/ocgate/).
Perryman, M. A. C., European Space Agency Space Science Department, and the Hipparcos Science Team. 1997, *The Hipparcos and Tycho Catalogues, ESA SP-1200* (VizieR On-line Data Catalog: I/239), ESA Publications Division, Noordwijk, The Netherlands.
Rigollet, R. 1953, *IAU Circ.*, No. 1387, 1.
Samec, R. G., Su, W., and Dewitt, J. R. 1993, *Publ. Astron. Soc. Pacific*, **105**, 1441.
Skrutskie, M. F., *et al.* 2006, *Astron. J.*, **131**, 1163.
U.S. Naval Observatory. 2012, UCAC-3 (http://www.usno.navy.mil/USNO/astrometry/optical-IR-prod/ucac). [VizieR On-line Data Catalog: I/315.]
Van Hamme, W. V., and Wilson, R. E. 1998, *Bull. Amer. Astron. Soc.*, **30**, 1402.
Vidal-Sainz, J., and Garcia-Melendo, E. 1996, *Inf. Bull. Var. Stars*, No. 4393, 1.
Wilson, R. E. 1990, *Astrophys. J.*, **356**, 613.
Wilson, R. E. 1994, *Publ. Astron. Soc. Pacific*, **106**, 921.
Wilson, R. E., and Devinney, E. J. 1971, *Astrophys. J.*, **166**, 605.
Wolf, M., and Diethelm, R. 1999, *BBSAG Bull.*, No. 125, 1.
Zejda, M. 2004, *Inf. Bull. Var. Stars*, No. 5583, 1.
Zhang, X. B., and Zhang, R. X. 2006, *New Astron.*, **11**, 339 (http://www.sciencedirect.com/science/article/pii/S1384107605001375).

Table 2. Observations of GQ CNC, ΔB, ΔV, ΔR_c, ΔI_c, variable-comparison.

Δ*B*	*HJD 2457270+*	Δ*B*	*HJD 2457270+*	Δ*B*	*HJD 2457270+*	Δ*B*	*HJD 2457270+*	Δ*B*	*HJD 2457270+*
2.189	90.6383	2.592	105.6499	1.748	106.6082	2.022	106.7419	1.789	108.7166
2.277	90.6420	2.560	105.6527	1.747	106.6116	1.991	106.7448	1.784	108.7087
2.353	90.6461	2.534	105.6556	1.778	106.6173	1.991	106.7448	1.791	108.7197
2.660	90.6601	2.434	105.6610	1.776	106.6210	1.933	106.7506	1.789	108.7227
2.596	90.6662	2.398	105.6638	1.795	106.6238	1.921	106.7534	1.793	108.7286
2.460	90.6726	2.338	105.6666	1.806	106.6266	1.856	106.7658	1.802	108.7317
2.385	90.6768	2.285	105.6698	1.819	106.6299	1.846	106.7687	1.807	108.7347
2.240	90.6836	2.251	105.6727	1.825	106.6327	1.837	106.7715	1.813	108.7405
2.061	90.6938	2.206	105.6755	1.832	106.6356	1.831	106.7747	1.825	108.7436
2.034	90.6966	2.117	105.6820	1.843	106.6411	1.818	106.7775	1.837	108.7467
1.951	90.7056	2.085	105.6849	1.853	106.6440	1.796	106.7803	1.853	108.7522
1.897	90.7084	2.057	105.6877	1.865	106.6468	1.787	106.7842	1.851	108.7552
1.878	90.7154	2.020	105.6909	1.873	106.6501	1.794	106.7870	1.866	108.7583
1.855	90.7216	2.001	105.6937	1.888	106.6529	2.413	108.6144	1.885	108.7637
1.844	90.7244	1.980	105.6966	1.904	106.6558	2.339	108.6175	1.910	108.7668
1.843	90.7280	1.955	105.7009	1.935	106.6594	2.299	108.6205	1.938	108.7699
1.811	90.7309	1.932	105.7038	1.962	106.6623	2.247	108.6242	1.981	108.7759
1.804	90.7369	1.915	105.7066	1.990	106.6651	2.190	108.6273	2.014	108.7790
1.784	90.7400	1.911	105.7098	2.093	106.6743	2.147	108.6303	2.050	108.7821
1.769	90.7461	1.907	105.7127	2.149	106.6771	2.104	108.6335	2.101	108.7859
1.734	90.7755	1.895	105.7155	2.190	106.6799	2.072	108.6366	2.157	108.7889
1.732	90.7783	1.875	105.7200	2.264	106.6839	2.035	108.6396	2.210	108.7920
1.741	90.7868	1.862	105.7229	2.314	106.6868	1.977	108.6468	1.934	119.6316
1.741	90.7897	1.858	105.7257	2.380	106.6896	1.945	108.6499	1.900	119.6383
1.758	90.8010	1.825	105.7432	2.445	106.6930	1.922	108.6529	1.886	119.6411
1.767	90.8045	1.821	105.7460	2.510	106.6958	1.896	108.6587	1.885	119.6443
1.779	90.8073	1.831	105.7489	2.580	106.6987	1.878	108.6618	1.844	119.6560
1.784	90.8102	1.820	105.7551	2.629	106.7020	1.871	108.6648	1.831	119.6649
1.784	90.8130	1.817	105.7601	2.674	106.7049	1.849	108.6712	1.823	119.6710
1.958	90.8368	1.809	105.7635	2.651	106.7077	1.843	108.6743	1.805	119.6766
1.983	90.8397	1.806	105.7673	2.605	106.7109	1.828	108.6774	1.802	119.6856
2.024	90.8425	1.806	105.7720	2.534	106.7137	1.824	108.6823	1.795	119.6943
2.147	105.6235	1.845	105.7787	2.482	106.7166	1.809	108.6854	1.806	119.6976
2.199	105.6263	1.795	105.7861	2.422	106.7198	1.810	108.6884	1.812	119.7004
2.267	105.6301	1.846	105.7904	2.352	106.7227	1.804	108.6939	1.822	119.7092
2.319	105.6329	1.890	105.7931	2.293	106.7255	1.795	108.6969	1.826	119.7153
2.376	105.6358	1.861	105.7959	2.203	106.7302	1.795	108.7000	1.842	119.7209
2.440	105.6389	1.863	105.7992	2.154	106.7331	1.784	108.7056	1.857	119.7272
2.490	105.6418	1.862	105.8019	2.110	106.7359	1.784	108.7087	1.945	119.7476
2.541	105.6446	1.883	105.8047	2.070	106.7391	1.786	108.7118	2.078	119.7613

Table continued on following pages

Table 2. Observations of GQ CNC, ΔB, ΔV, ΔR_c, ΔI_c, variable-comparison, cont.

ΔV	HJD 2457270+	ΔV	HJD 2457270+	ΔV	HJD 2457270+	ΔV	HJD 2457270+	ΔV	HJD 2457270+
2.480	90.6390	2.045	90.8053	2.078	105.7728	2.403	108.6313	2.165	119.6391
2.554	90.6428	2.046	90.8081	2.089	105.7795	2.364	108.6344	2.155	119.6419
2.636	90.6470	2.060	90.8110	1.866	105.7869	2.327	108.6375	2.129	119.6451
2.726	90.6508	2.265	105.6169	2.097	105.7912	2.288	108.6406	2.114	119.6479
2.798	90.6536	2.285	105.6182	2.109	105.7939	2.227	108.6477	2.126	119.6507
2.876	90.6581	2.381	105.6243	2.111	105.7966	2.203	108.6508	2.104	119.6540
2.901	90.6609	2.428	105.6271	2.117	105.8000	2.179	108.6539	2.116	119.6568
2.810	90.6675	2.492	105.6309	2.138	105.8027	2.160	108.6596	2.099	119.6596
2.685	90.6739	2.543	105.6337	2.133	105.8054	2.146	108.6627	2.093	119.6629
2.607	90.6776	2.596	105.6366	2.051	106.6054	2.136	108.6658	2.088	119.6657
2.525	90.6816	2.656	105.6397	2.038	106.6090	2.114	108.6721	2.086	119.6685
2.469	90.6844	2.712	105.6426	2.045	106.6125	2.105	108.6752	2.079	119.6718
2.413	90.6881	2.762	105.6454	2.053	106.6182	2.100	108.6783	2.072	119.6746
2.365	90.6910	2.792	105.6507	2.065	106.6218	2.083	108.6832	2.074	119.6774
2.309	90.6946	2.762	105.6535	2.073	106.6246	2.083	108.6863	2.051	119.6807
2.281	90.6974	2.715	105.6564	2.081	106.6275	2.076	108.6894	2.052	119.6835
2.199	90.7064	2.632	105.6618	2.087	106.6307	2.068	108.6948	2.046	119.6864
2.187	90.7092	2.580	105.6646	2.097	106.6335	2.062	108.6979	2.054	119.6895
2.135	90.7162	2.526	105.6674	2.103	106.6364	2.060	108.7009	2.031	119.6923
2.129	90.7190	2.481	105.6707	2.113	106.6419	2.055	108.7066	2.051	119.6951
2.116	90.7224	2.439	105.6735	2.123	106.6448	2.061	108.7097	2.051	119.6984
2.114	90.7253	2.392	105.6764	2.131	106.6476	2.057	108.7127	2.068	119.7012
2.102	90.7289	2.313	105.6828	2.143	106.6509	2.060	108.7175	2.078	119.7040
2.087	90.7317	2.282	105.6857	2.155	106.6537	2.054	108.7206	2.072	119.7071
2.064	90.7349	2.255	105.6885	2.171	106.6566	2.055	108.7236	2.079	119.7100
2.063	90.7377	2.234	105.6917	2.204	106.6602	2.065	108.7295	2.081	119.7128
2.049	90.7408	2.215	105.6946	2.229	106.6631	2.076	108.7326	2.086	119.7161
2.051	90.7436	2.185	105.6974	2.255	106.6659	2.066	108.7357	2.090	119.7189
2.038	90.7469	2.163	105.7017	2.370	106.6751	2.084	108.7414	2.082	119.7217
2.033	90.7497	2.140	105.7046	2.408	106.6779	2.096	108.7445	2.105	119.7252
2.027	90.7528	2.136	105.7074	2.458	106.6807	2.102	108.7476	2.110	119.7280
2.020	90.7556	2.125	105.7107	2.536	106.6847	2.111	108.7531	2.122	119.7308
2.022	90.7590	2.114	105.7135	2.583	106.6876	2.115	108.7562	2.118	119.7340
2.019	90.7618	2.120	105.7163	2.644	106.6904	2.117	108.7592	2.137	119.7368
2.012	90.7646	2.098	105.7209	2.704	106.6938	2.147	108.7646	2.144	119.7397
2.009	90.7675	2.096	105.7237	2.765	106.6967	2.171	108.7677	2.157	119.7427
2.011	90.7703	2.088	105.7265	2.826	106.6995	2.198	108.7708	2.185	119.7456
2.018	90.7731	2.079	105.7311	2.891	106.7028	2.244	108.7769	2.203	119.7484
2.023	90.7763	2.076	105.7350	2.896	106.7057	2.285	108.7799	2.229	119.7519
2.016	90.7791	2.064	105.7369	2.873	106.7085	2.318	108.7830	2.252	119.7547
2.029	90.7820	2.061	105.7393	2.825	106.7117	2.371	108.7868	2.288	119.7575
2.023	90.7848	2.061	105.7440	2.765	106.7145	2.408	108.7899	2.341	119.7621
2.017	90.7876	2.054	105.7469	2.702	106.7174	2.474	108.7929	2.374	119.7649
2.023	90.7905	2.054	105.7497	2.658	108.6153	2.312	119.6186	2.428	119.7678
2.027	90.7933	2.049	105.7557	2.595	108.6184	2.219	119.6268		
2.018	90.7961	2.070	105.7607	2.538	108.6215	2.205	119.6296		
2.033	90.7990	2.054	105.7640	2.494	108.6251	2.184	119.6325		
2.043	90.8018	2.076	105.7678	2.448	108.6282	2.169	119.6363		

Table continued on following pages

Table 2. Observations of GQ CNC, ΔB, ΔV, ΔR_c, ΔI_c, variable-comparison, cont.

ΔR_c	HJD 2457270+	ΔR_c	HJD 2457270+	ΔR_c	HJD 2457270+	ΔR_c	HJD 2457270+	ΔR_c	HJD 2457270+
2.618	90.6406	2.203	90.8173	2.237	105.7980	2.248	106.7608	2.350	108.7775
2.694	90.6448	2.216	90.8202	2.242	105.8008	2.235	106.7645	2.386	108.7806
2.774	90.6486	2.227	90.8230	2.258	105.8035	2.224	106.7673	2.455	108.7844
2.845	90.6514	2.251	90.8263	2.166	106.6069	2.218	106.7701	2.494	108.7875
2.941	90.6559	2.275	90.8291	2.167	106.6097	2.208	106.7733	2.544	108.7905
2.990	90.6587	2.305	90.8326	2.164	106.6105	2.199	106.7761	2.358	119.6247
2.979	90.6639	2.328	90.8354	2.175	106.6131	2.194	106.7790	2.340	119.6275
2.860	90.6707	2.358	90.8383	2.175	106.6160	2.183	106.7828	2.325	119.6303
2.766	90.6754	2.473	105.6221	2.184	106.6196	2.184	106.7857	2.302	119.6341
2.683	90.6795	2.520	105.6250	2.185	106.6224	2.809	108.6129	2.281	119.6369
2.622	90.6823	2.574	105.6287	2.190	106.6253	2.761	108.6160	2.269	119.6397
2.559	90.6860	2.616	105.6316	2.200	106.6285	2.705	108.6191	2.263	119.6429
2.509	90.6888	2.673	105.6344	2.206	106.6314	2.647	108.6227	2.255	119.6458
2.455	90.6924	2.734	105.6375	2.213	106.6342	2.600	108.6258	2.238	119.6486
2.419	90.6952	2.781	105.6404	2.229	106.6398	2.553	108.6289	2.244	119.6519
2.325	90.7042	2.838	105.6432	2.229	106.6426	2.514	108.6320	2.228	119.6547
2.306	90.7070	2.913	105.6485	2.239	106.6454	2.474	108.6351	2.229	119.6575
2.263	90.7140	2.901	105.6514	2.254	106.6487	2.440	108.6382	2.224	119.6608
2.249	90.7168	2.870	105.6542	2.260	106.6516	2.370	108.6453	2.213	119.6636
2.241	90.7202	2.778	105.6596	2.273	106.6544	2.344	108.6484	2.195	119.6664
2.227	90.7231	2.736	105.6624	2.300	106.6581	2.321	108.6515	2.195	119.6696
2.228	90.7267	2.694	105.6653	2.325	106.6609	2.287	108.6572	2.204	119.6724
2.212	90.7295	2.591	105.6713	2.350	106.6637	2.269	108.6603	2.186	119.6753
2.196	90.7327	2.551	105.6742	2.451	106.6729	2.255	108.6634	2.206	119.6785
2.203	90.7355	2.461	105.6807	2.492	106.6757	2.249	108.6697	2.193	119.6814
2.178	90.7387	2.428	105.6835	2.532	106.6786	2.231	108.6728	2.192	119.6842
2.176	90.7415	2.399	105.6863	2.598	106.6826	2.231	108.6759	2.168	119.6874
2.171	90.7447	2.376	105.6895	2.648	106.6854	2.214	108.6808	2.175	119.6902
2.167	90.7475	2.348	105.6924	2.697	106.6883	2.210	108.6839	2.184	119.6930
2.152	90.7507	2.324	105.6952	2.767	106.6916	2.209	108.6870	2.177	119.6962
2.148	90.7535	2.300	105.6996	2.819	106.6945	2.191	108.6924	2.195	119.6990
2.140	90.7569	2.275	105.7024	2.892	106.6973	2.193	108.6955	2.194	119.7019
2.142	90.7597	2.262	105.7053	2.954	106.7007	2.186	108.6985	2.189	119.7050
2.128	90.7625	2.257	105.7085	3.010	106.7035	2.180	108.7042	2.201	119.7078
2.141	90.7653	2.246	105.7113	3.009	106.7063	2.181	108.7072	2.223	119.7106
2.134	90.7682	2.244	105.7142	2.966	106.7095	2.184	108.7103	2.207	119.7139
2.131	90.7710	2.228	105.7187	2.913	106.7124	2.182	108.7151	2.210	119.7168
2.139	90.7741	2.225	105.7215	2.853	106.7152	2.178	108.7182	2.228	119.7196
2.139	90.7770	2.218	105.7244	2.786	106.7185	2.176	108.7212	2.238	119.7231
2.128	90.7798	2.188	105.7418	2.728	106.7213	2.187	108.7271	2.229	119.7259
2.139	90.7826	2.181	105.7447	2.670	106.7242	2.190	108.7302	2.241	119.7287
2.137	90.7855	2.173	105.7475	2.580	106.7289	2.186	108.7333	2.237	119.7318
2.138	90.7883	2.173	105.7542	2.537	106.7317	2.190	108.7390	2.252	119.7347
2.136	90.7912	2.186	105.7590	2.489	106.7345	2.174	108.7421	2.257	119.7375
2.145	90.7939	2.181	105.7625	2.445	106.7377	2.198	108.7452	2.271	119.7406
2.148	90.7968	2.177	105.7664	2.412	106.7406	2.222	108.7507	2.279	119.7434
2.155	90.7996	2.182	105.7708	2.383	106.7434	2.231	108.7538	2.307	119.7462
2.167	90.8031	2.181	105.7775	2.351	106.7464	2.234	108.7568	2.331	119.7497
2.165	90.8059	2.212	105.7849	2.323	106.7493	2.236	108.7622	2.357	119.7526
2.172	90.8089	2.218	105.7892	2.298	106.7521	2.273	108.7653	2.381	119.7554
2.183	90.8117	2.215	105.7920	2.271	106.7551	2.274	108.7684	2.434	119.7600
2.189	90.8145	2.225	105.7947	2.267	106.7580	2.332	108.7744		

Table continued on next page

Table 2. Observations of GQ CNC, ΔB, ΔV, ΔR, ΔI, variable-comparison, cont.

ΔI_c	HJD 2457270+	ΔI_c	HJD 2457270+	ΔI_c	HJD 2457270+	ΔI_c	HJD 2457270+	ΔI_c	HJD 2457270+
2.811	90.6454	2.329	90.8207	2.340	105.7953	2.339	106.7614	2.379	108.7690
2.893	90.6492	2.354	90.8235	2.334	105.7986	2.330	106.7651	2.426	108.7750
2.956	90.6520	2.365	90.8268	2.354	105.8013	2.327	106.7679	2.431	108.7781
3.040	90.6565	2.392	90.8297	2.367	105.8041	2.320	106.7707	2.483	108.7812
3.113	90.6593	2.410	90.8332	2.264	106.6074	2.312	106.7739	2.559	108.7850
3.064	90.6649	2.448	90.8360	2.281	106.6109	2.300	106.7767	2.598	108.7880
2.941	90.6715	2.480	90.8389	2.270	106.6137	2.302	106.7795	2.461	119.6252
2.842	90.6760	2.513	90.8417	2.284	106.6166	2.280	106.7834	2.438	119.6281
2.769	90.6800	2.578	105.6227	2.287	106.6202	2.283	106.7862	2.420	119.6309
2.710	90.6829	2.626	105.6255	2.292	106.6230	2.271	106.7891	2.400	119.6347
2.645	90.6866	2.683	105.6293	2.305	106.6259	2.906	108.6135	2.389	119.6375
2.599	90.6894	2.741	105.6321	2.304	106.6291	2.856	108.6166	2.375	119.6403
2.552	90.6930	2.788	105.6350	2.315	106.6320	2.809	108.6196	2.367	119.6435
2.513	90.6958	2.848	105.6381	2.320	106.6348	2.749	108.6233	2.364	119.6463
2.422	90.7048	2.904	105.6410	2.329	106.6404	2.694	108.6264	2.339	119.6491
2.406	90.7076	2.955	105.6438	2.335	106.6432	2.655	108.6294	2.347	119.6524
2.363	90.7146	3.021	105.6491	2.347	106.6460	2.613	108.6326	2.337	119.6553
2.355	90.7174	3.000	105.6519	2.361	106.6493	2.576	108.6357	2.334	119.6581
2.345	90.7208	2.960	105.6548	2.366	106.6521	2.534	108.6387	2.327	119.6613
2.329	90.7237	2.877	105.6602	2.383	106.6550	2.460	108.6459	2.325	119.6641
2.319	90.7273	2.829	105.6630	2.411	106.6587	2.441	108.6490	2.316	119.6670
2.317	90.7301	2.774	105.6659	2.435	106.6615	2.420	108.6521	2.312	119.6702
2.314	90.7333	2.717	105.6691	2.459	106.6643	2.420	108.6521	2.304	119.6730
2.300	90.7361	2.681	105.6719	2.564	106.6735	2.381	108.6578	2.326	119.6758
2.293	90.7392	2.640	105.6748	2.601	106.6763	2.366	108.6609	2.293	119.6791
2.289	90.7421	2.556	105.6812	2.642	106.6791	2.360	108.6639	2.294	119.6820
2.285	90.7453	2.522	105.6841	2.708	106.6831	2.351	108.6703	2.302	119.6848
2.285	90.7481	2.493	105.6869	2.760	106.6860	2.340	108.6734	2.285	119.6879
2.269	90.7513	2.469	105.6901	2.809	106.6888	2.328	108.6765	2.279	119.6908
2.257	90.7541	2.442	105.6930	2.876	106.6922	2.322	108.6814	2.284	119.6936
2.250	90.7574	2.422	105.6958	2.942	106.6951	2.318	108.6845	2.287	119.6968
2.261	90.7602	2.392	105.7001	2.988	106.6979	2.313	108.6875	2.300	119.6996
2.254	90.7631	2.378	105.7030	3.068	106.7012	2.300	108.6930	2.305	119.7024
2.250	90.7659	2.366	105.7058	3.101	106.7041	2.295	108.6960	2.302	119.7056
2.248	90.7687	2.357	105.7091	3.093	106.7069	2.296	108.6991	2.305	119.7084
2.252	90.7715	2.346	105.7119	3.042	106.7101	2.290	108.7048	2.306	119.7112
2.256	90.7747	2.343	105.7147	2.975	106.7130	2.285	108.7078	2.311	119.7145
2.251	90.7775	2.333	105.7193	2.929	106.7158	2.290	108.7109	2.324	119.7173
2.248	90.7804	2.330	105.7221	2.863	106.7191	2.292	108.7157	2.335	119.7201
2.256	90.7832	2.319	105.7250	2.802	106.7219	2.290	108.7187	2.333	119.7236
2.259	90.7860	2.291	105.7424	2.744	106.7247	2.300	108.7218	2.351	119.7264
2.251	90.7889	2.286	105.7453	2.667	106.7294	2.295	108.7277	2.343	119.7293
2.257	90.7917	2.286	105.7481	2.617	106.7323	2.295	108.7308	2.352	119.7324
2.271	90.7945	2.287	105.7546	2.581	106.7351	2.295	108.7338	2.357	119.7352
2.269	90.7974	2.282	105.7595	2.535	106.7383	2.287	108.7396	2.377	119.7381
2.271	90.8002	2.285	105.7629	2.505	106.7411	2.314	108.7427	2.384	119.7412
2.285	90.8037	2.284	105.7668	2.471	106.7440	2.279	108.7458	2.404	119.7440
2.285	90.8065	2.303	105.7714	2.430	106.7470	2.294	108.7513	2.423	119.7468
2.296	90.8094	2.309	105.7781	2.409	106.7498	2.332	108.7543	2.450	119.7503
2.289	90.8122	2.324	105.7855	2.397	106.7527	2.313	108.7574	2.471	119.7531
2.301	90.8151	2.326	105.7898	2.376	106.7557	2.349	108.7628		
2.321	90.8179	2.330	105.7925	2.359	106.7586	2.371	108.7659		

Table 3. O–C residuals, linear and quadratic period study, GQ Cnc.

	Epoch	Cycles	Lineal Residuals	Quadratic Residuals	Wt.	Reference
1	50154.4206	–14808.5	–0.0060	–0.0054	1.0	Vidal-Sainz and Garcia-Melendo 1996
2	50159.4876	–14796.5	–0.0055	–0.0049	1.0	Vidal-Sainz and Garcia-Melendo 1996
3	50164.3426	–14785.0	–0.0059	–0.0053	1.0	Vidal-Sainz and Garcia-Melendo 1996
4	50165.3996	–14782.5	–0.0044	–0.0038	1.0	Vidal-Sainz and Garcia-Melendo 1996
5	50207.4174	–14683.0	0.0036	0.0042	1.0	Vidal-Sainz and Garcia-Melendo 1996
6	50218.3948	–14657.0	0.0036	0.0041	1.0	Vidal-Sainz and Garcia-Melendo 1996
7	50226.4173	–14638.0	0.0041	0.0047	1.0	Vidal-Sainz and Garcia-Melendo 1996
8	51199.6080	–12333.0	0.0035	0.0032	1.0	Wolf and Diethelm 1999
9	51274.3380	–12156.0	0.0025	0.0022	1.0	Paschke 1999
10	51984.4940	–10474.0	0.0033	0.0026	1.0	Blättler *et al.* 2001
11	52279.6194	–9775.0	0.0048	0.0039	1.0	Zejda 2004
12	52362.3700	–9579.0	0.0024	0.0015	1.0	Locher *et al.* 2002
13	52691.2705	–8800.0	0.0023	0.0013	1.0	Diethelm 2003
14	53325.6310	–7297.5	–0.0060	–0.0071	0.5	Locher 2005
15	54839.8837	–3711.0	–0.0051	–0.0059	1.0	Diethelm 2009
16	54842.8436	–3704.0	–0.0007	–0.0015	1.0	Diethelm 2009
17	55245.8432	–2749.5	0.0006	0.0000	1.0	Diethelm 2010
18	55275.3979	–2679.5	0.0007	0.0001	1.0	Hübscher and Monninger 2011
19	55577.9104	–1963.0	0.0006	0.0002	1.0	Diethelm 2009
20	55652.6406	–1786.0	–0.0002	–0.0005	1.0	Diethelm 2009
21	56002.6490	–957.0	–0.0029	–0.0029	0.5	Diethelm 2012
22	56390.6620	–38.0	0.0002	0.0005	1.0	Present Observations
23	56405.6505	–2.5	0.0003	0.0006	1.0	Present Observations
24	56406.7056	0.0	–0.0002	0.0002	1.0	Present Observations
25	57414.3070	2386.5	0.0000	0.0014	1.0	Hübscher 2017
26	57414.5183	2387.0	0.0001	0.0016	1.0	Hübscher 2017

Table 4. Light curve characteristics, GQ Cnc.

Filter	Phase	Magnitude Min. I	Phase	Magnitude Max. II
	0.0		0.25	
B		2.991 ± 0.005		2.135 ± 0.005
V		3.092 ± 0.003		2.252 ± 0.003
R_c		2.991 ± 0.026		2.135 ± 0.005
I_c		3.092 ± 0.027		2.252 ± 0.003
Filter	*Phase*	*Magnitude Min. II*	*Phase*	*Magnitude Max. I*
	0.50		0.75	
B		2.907 ± 0.026		2.179 ± 0.005
V		3.011 ± 0.027		2.286 ± 0.003
R_c		2.907 ± 0.026		2.179 ± 0.005
I_c		3.011 ± 0.027		2.286 ± 0.003
Filter		*Min. I – Max. II*		*Min. I – Min. II*
B		0.856 ± 0.009		0.084 ± 0.031
V		0.840 ± 0.007		0.081 ± 0.031
R_c		0.856 ± 0.031		0.084 ± 0.053
I_c		0.840 ± 0.031		0.081 ± 0.054
Filter		*Max. I – Max. II*		
B		0.044 ± 0.009		
V		0.034 ± 0.007		
R_c		0.044 ± 0.009		
I_c		0.034 ± 0.007		

Table 5. GQ Cnc light curve solutions.

Parameters	*Best Solution*	*Initial Solution*
λ_B, λ_V, λ_R, λ_I (nm)	440, 550, 640, 790	—
$x_{bol1,2}$, $y_{bol1,2}$	0.648 0 .647, 0.207, 0 .176	—
$x_{1I,2I}$, $y_{1I,2I}$	0.590, 0. 590, 0.260, 0.260	—
$x_{1R,2R}$, $y_{1R,2R}$	0. 674, 0.674, 0. 269, 0. 269	—
$x_{1V,2V}$, $y_{1V,2V}$	0.745, 0.745, 0. 256, 0. 256	—
$x_{1B,2B}$, $y_{1B,2B}$	0. 829, 0.829, 0.185, 0.185	—
g_1 , g_2	0.320,0.320	—
A_1 , A_2	0.5, 0.5	—
Inclination (°)	85.6 ± 0.1	85.21 ± 0.15
T_1, T_2 (K)	5250*, 5247 ± 2	5250, 5225 ± 1
Ω_1, Ω_2 pot	3.529 ± 0.002, 3.442 ± 0.002	3.7549 ± 0.0013, 3.804 ± 0.002
q (m_2 / m_1)	0.802 ± 0.001	0.9877 ± 0.0004
Fill-outs: F_1, F_2 (%)	97, 99	94, 98
L_1 / (L_1 + L_2)I	0.5326 ± 0.00009	0.518 ± 0.001
L_1 / (L_1 + L_2)R	0.5327 ± 0.0010	0.519 ± 0.001
L_1 / (L_1 + L_2)V	0.5326 ± 0.0011	0.5199 ± 0.0006
L_1 / (L_1 + L_2)B	0.5327 ± 0.0008	0.5218 ± 0.0008
JD_o (days)	2456406.70555 ± .000011	2456406.70552 ± .000005
Period (days)	0. 4222380 ± 0.0000003	0. 42223823 ± 0.0000003
r_1, r_2 (pole)	0. 3604 ± 0.0035, 0.335 ± 0.004	0. 354 ± 0.001, 0.346 ± 0.004
r_1, r_2 (point)	0.439 ± 0.011, 0.4405 ± 0.0256	0.463 ± 0.024, 0.433 ± 0.017
r_1, r_2 (side)	0.377 ± 0.004, 0.351 ± 0.004	0.372 ± 0.004, 0.362 ± 0.005
r_1, r_2 (back)	0.402 ± 0.006, 0.381 ± 0.006	0.401 ± 0.006, 0.389 ± 0.007
Spot Parameters	*Star 1*	*Hot Spot*
Colatitude (°)	24 ± 1	94 ± 2
Longitude (°)	238 ± 1	224 ± 1
Spot radius (°)	11.7 ± 0.2	15.1 ± 0.5
Tfact	1.47 ± 0.01	1.106 ± 0.006
$\Sigma(res)^2$	0.7842	0.8303

**The primary temperature is an estimate from 2MASS results ± 150 K.*